IEEE Access
Multidisciplinary | Rapid Review | Open Access Journal

Received May 31, 2019, accepted June 15, 2019, date of publication June 20, 2019, date of current version July 9, 2019.

Digital Object Identifier 10.1109/ACCESS.2019.2924022

A Compact Dual-Broadband Multiple-Input Multiple-Output (MIMO) Indoor Base Station Antenna for 2G/3G/LTE Systems

YAN ZHAO[1], (Senior Member, IEEE),
CHAWALIT RAKLUEA[2,3], (Graduate Student Member, IEEE),
TANAN HONGNARA[4], (Member, IEEE), AND
SARAWUTH CHAIMOOL[5], (Senior Member, IEEE)

[1]International School of Engineering, Faculty of Engineering, Chulalongkorn University, Bangkok 10330, Thailand
[2]Department of Electrical and Computer Engineering, King Mongkut's University of Technology North Bangkok, Bangkok 10800, Thailand
[3]Department of Electronic and Telecommunication Engineering, Faculty of Engineering, Rajamangala University of Technology Thanyaburi, Khlong Hok 12110, Thailand
[4]Denki Kogyo Company Ltd., Tokyo 100-0005, Japan
[5]Department of Electrical Engineering, Faculty of Engineering, Khon Kaen University, Khon Kaen 40002, Thailand

Corresponding author: Yan Zhao (yan.z@chula.ac.th)

This work was supported by the Thailand Research Fund (TRF) under Grant RSA5980051.

ABSTRACT In this paper, we propose a dual-broadband multiple-input multiple-output (MIMO) indoor base station antenna for 2G/3G/LTE systems. The proposed MIMO antenna has a low profile with its overall dimensions of $220 \times 220 \times 42$ mm^3 and utilizes both spatial and polarization diversities. The antenna operates at 800–960 and 1700–2700 MHz simultaneously, with the return loss of higher than 14 dB across both frequency bands. The isolations of the antenna are 18 and 25 dB, with antenna gains of 3.6 and 7.2 dBi for the lower and upper frequency bands, respectively. The proposed MIMO antenna is designed and fabricated with its practical deployment in mind, such as the durability and overall low cost. Comparing with existing commercial 2G/3G/LTE antennas, our proposed design offers a more compact size and simpler feeding structure.

INDEX TERMS Base station antenna, long term evolution (LTE), multiple-input multiple-output (MIMO).

I. INTRODUCTION

The rapid development of mobile communication technology has placed higher and higher demand on the requirement of wireless communication devices for achieving faster data processing and lower bit error rate. In terms of antennas as an essential part of wireless communication systems, they are required to provide reliable wireless links, as well as have low cost and low profiles, especially for the case of indoor base stations. Although the fifth generation (5G) mobile system is already on its way to be deployed, a large portion of existing mobile networks is still based on 2G, 3G or 4G long-term evolution (LTE) systems. Thus the design of antennas to operate at 700, 750, 800, 850, 900, 1900, 1700/2100, 2500 and 2600 MHz bands (depending on the country's regulation) is still desirable to fully take advantage of advanced wireless communication technology.

The associate editor coordinating the review of this manuscript and approving it for publication was Luyu Zhao.

The majority of existing commercial indoor base station antennas covering 2G/3G/LTE frequencies are either the monopole or dipole type [1]–[6], thus the height of the antenna is large (> 10 cm) and the antenna gain is not very high. Specifically, by combining a monopole as a vertically polarized (VP) element and printed dipoles as horizontally polarized (HP) elements [1]–[5], a dual-polarized antenna can be realized for 2G/3G/LTE indoor base stations covering both frequency ranges of 800 - 960 and 1700 - 2700 MHz. However, these proposed designs require complex feeding networks or diplexers etc., and only the VP or HP element can cover the upper frequency band in most designs.

To realize more compact 2G/3G/LTE indoor base station antennas, the microstrip-type radiators are typically used. A dual-polarized patch antenna is proposed in [7] for 1900 - 2700 MHz, and a slot-coupled stacked-patch array antenna is introduced in [8] for 1700 - 2700 MHz. For dual-wideband operations, a dual-broadband planar antenna for 800 - 980 MHz and 1540 - 2860 MHz is presented in [9],

however, the antenna needs to be separately fed for lower and upper band operations. A double-layer magnetoelectric dipole antenna is proposed in [10] for 790 - 1010 MHz and 1380 - 2780 MHz, while the size of the antenna is large and it requires a complicated fabrication process.

Intrinsically, microstrip-type antennas have narrow operating bandwidth. Typical techniques to increase bandwidth of microstrip antennas include cutting corners of the radiating patch to create additional resonant modes [11], stacking an additional (parasitic) patch to introduce a second resonance [12]–[19], cutting a U-shaped slot on the radiating patch to direct the flow of surface currents [17], [20]–[25], adding shorting pins [21], [26], and a combination of the above techniques etc. [27]–[29].

In addition to meeting the bandwidth requirement of 2G/3G/LTE systems, to further increase channel capacity, multiple-input multiple-output (MIMO) antennas are usually desirable. In this paper, based on our previous design of a microstrip-type dual-wideband element [30], we propose a MIMO indoor base station antenna utilizing spatial and polarization diversities for 2G/3G/LTE systems operating at 800 - 960 MHz and 1700 - 2700 MHz simultaneously. Furthermore, practical issues such as maintaining a low cost and durability of materials, input power rating, as well as meeting the passive intermodulation (PIM) requirement in industry have been taken into consideration in our design. It is worth mentioning that the MIMO antenna proposed in this paper has already been manufactured in a large quantity and is currently being used in several local mobile networks.

II. ANTENNA DESIGN AND FABRICATION

The design evolution of the proposed 2G/3G/LTE MIMO antenna can be summarized as follows. The complete design contains two identical single elements, with each element covering the required frequency bands of 800 - 960 MHz (lower band) and 1700 - 2700 MHz (upper band), as shown in Fig. 1(a). For each element, we combine two types of antenna structures into a single two-level 'composite' antenna: a microstrip patch antenna with multiple slots on the top level for the upper band (see Fig. 1(b)), and two monopole antennas on the lower level for the lower frequency band (see Fig. 1(c)). On the top patch, two additional slots are created to introduce two more resonances in addition to the intrinsic resonance of the microstrip patch, and two lower monopoles are folded to reduce the overall dimensions of each MIMO element.

In order to achieve a large impedance bandwidth using microstrip antennas, an 'air' substrate between ground and the radiating patch is usually used, since any dielectric materials used as substrate can lower the bandwidth of antenna. In our design, we keep a large height of 35 mm between the top radiating patch and the ground plane. For covering the upper frequency band of 1700 - 2700 MHz, we introduce multiple resonances to the top radiating patch by cutting two U-shaped slots facing each other, as shown in Fig. 1(b).

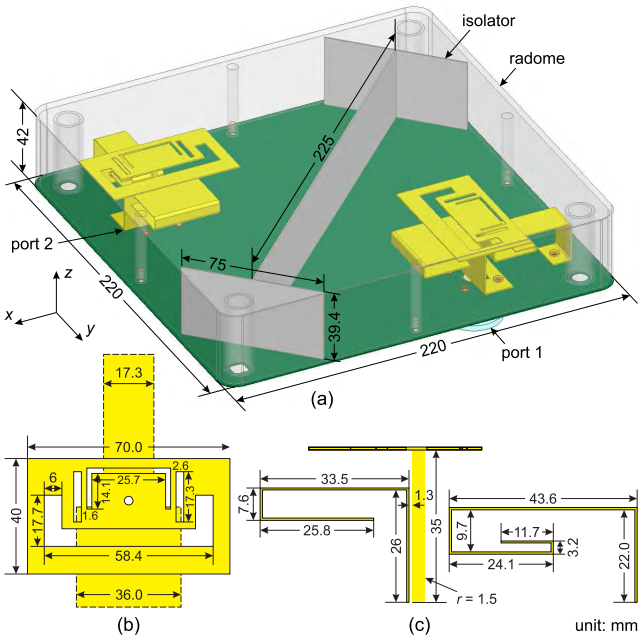

FIGURE 1. Geometry of the proposed MIMO indoor base station antenna for 2G/3G/LTE systems. (a) Perspective view of the design. (b) Top view of one antenna element with dimensions. (c) Side view of one antenna element with dimensions.

Initially, the overall length of each slot is chosen as one half-wavelength at the resonant frequency, and then the final slot dimensions are acquired through optimizations. The width of the slot also affects the resonant frequency and operating bandwidth, i.e. the larger the slot width, the lower the resonant frequency and the larger the operating bandwidth. In addition, two straight slots are added for the purpose of isolating current flows around the two U-shaped slots and improving impedance matching. For the lower frequency band of 800 - 960 MHz, two resonances are required and introduced by two folded monopoles, which are excited by edge coupling from the top radiating patch [31] and the coupling from the vertical feeding pin [32], as shown in Fig. 1(c). The total length of each folded monopole is approximately a quarter-wavelength at the resonant frequency, and the final dimensions of the monopoles are also obtained through optimizations. The distance between the feeding pin and the wider monopole, and the distance between the top radiating patch and the narrower monopole are critical parameters for achieving impedance matching at the lower frequency band. Figure 1(a) shows the overall structure of the proposed MIMO antenna with two elements (port 1 and port 2) oriented at an angle of 90 degrees between each other for realizing spatial and polarization diversities. A vertical metallic isolator is placed between two MIMO elements for improving both port isolation and impedance matching. As it is also shown in Fig. 1(a), a radome (assumed to be the acrylonitrile butadiene styrene (ABS) material with dielectric constant of 2.8) and small metallic screws are also included when modeling the antenna in simulations for practical considerations toward manufacturing.

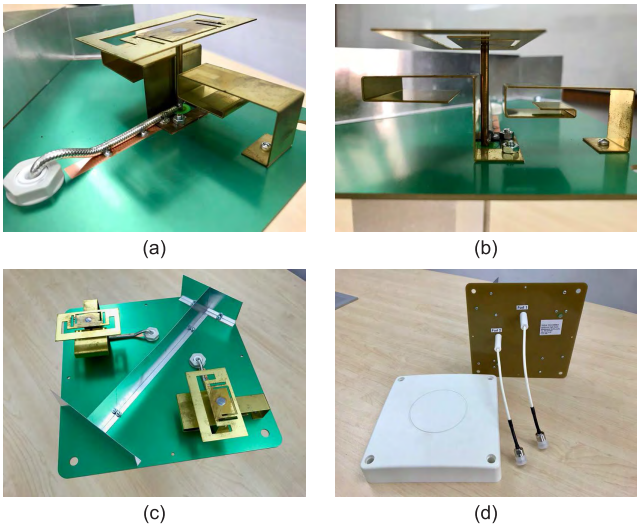

FIGURE 2. Photos of the fabricated indoor MIMO base station antenna for 2G/3G/LTE systems. (a) Perspective view. (b) Radome and back of the antenna. (c) Details of one antenna element and the feeding cable. (d) Side view of one antenna element.

In commercial indoor base station antennas, printed circuit boards (PCBs) are typically used as ground plane for rapid manufacturing and reducing cost of the product. In our design, a PCB with green protection film to avoid oxidation during operations is used. Some parts of the protection film are removed to enable the contact with antenna elements, the metallic isolator and the feeding cable, as shown in Fig. 2(a). Brass is chosen as the material for antenna elements due to its rigidness, and the thickness of all parts of the elements is 0.6 mm. It is important to model the thickness of the brass sheets accurately in simulations since it considerably affects the antenna's impedance matching. All radiating parts of the antenna are manufactured by metal sheet stamping and the lower components are folded by machine according to the dimensions shown in Fig. 1(c). The top radiating patch is soldered to the feeding pin and the feeding pin is firmly attached to the PCB ground. The lower folded elements are fixed to the PCB ground using stainless screws and aluminum rivets, as shown in Fig. 2(b). It is crucial that all horizontal parts are parallel to the PCB ground to achieve a good impedance matching. For the feeding structure, as most commercial indoor base station antennas use the so-called 'pigtail' style N-type connector, we also choose such connectors in the fabrication of our design, and thus the antenna is fed at the bottom of the feeding pin just above the PCB ground as shown in Fig. 2(a), which is different from the configuration in simulations with excitation ports below the ground. The outer layer of the cable is soldered to the PCB ground for stabilization and firm contact. The material of the metal isolator is chosen as aluminum for easy manufacturing and lowering the overall cost of antenna. The whole MIMO antenna is concealed in a radome made of ABS material and manufactured by an industry's standard process.

The comparisons of scattering (S-) parameters from simulations using the finite element method (FEM) and

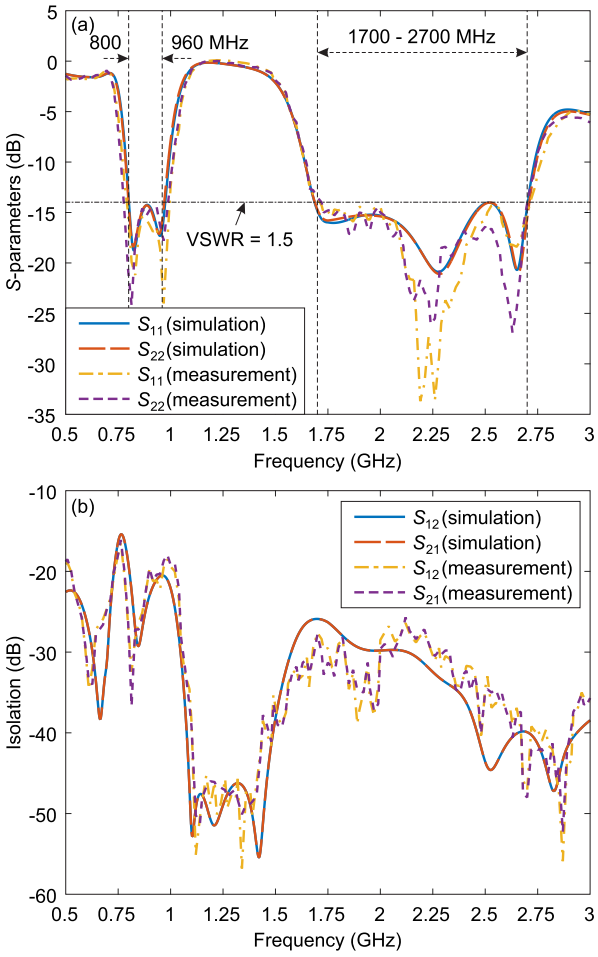

FIGURE 3. Comparisons of S-parameters of the proposed 2G/3G/LTE MIMO indoor base station antenna from simulation and measurement: (a) S_{11} and S_{22}, (b) isolation.

measurement in an anechoic chamber are shown in Fig. 3. It is clearly visible that two and three resonances are created covering the lower and upper frequency bands of 800 - 960 MHz and 1700 - 2700 MHz, respectively. The horizontal dashed line marks the value of −14 dB, equivalent to the voltage standing wave ratio (VSWR) of 1.5, which is a typical requirement from mobile network operators. It is also shown that the measurement results agree well with simulations which validates our design. The isolation of the MIMO antenna is shown in Fig. 3(b). It can be seen that isolations of 18 dB and 25 dB can be achieved for the lower and upper frequency bands, respectively.

To further explain the operating mechanism of the proposed MIMO antenna, the distributions of surface current at five resonant frequencies: 825 MHz, 950 MHz, 1750 MHz, 2280 MHz, and 2650 MHz from simulations are plotted and shown in Fig. 4. It is evident that two lower monopoles (Figs. 4(a) and (b)) resonate at their design frequencies to cover the lower frequency band of 800 - 960 MHz. While for the upper frequency band of 1700 - 2700 MHz, the resonance of the entire patch (Fig. 4(c)), the resonance of the larger U-shaped slot (Fig. 4(d)), and the resonance of the smaller U-shaped slot (Fig. 4(e)) are combined together.

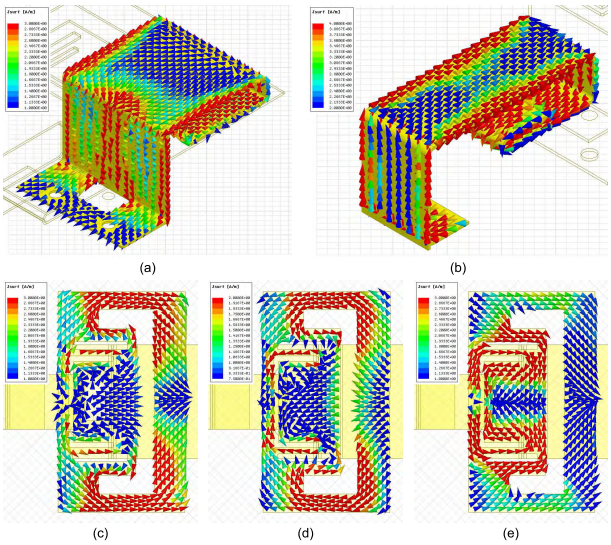

FIGURE 4. Distributions of surface current of the proposed 2G/3G/LTE MIMO indoor base station antenna at: (a) 825 MHz, (b) 950 MHz, (c) 1750 MHz, (d) 2280 MHz, and (e) 2650 MHz.

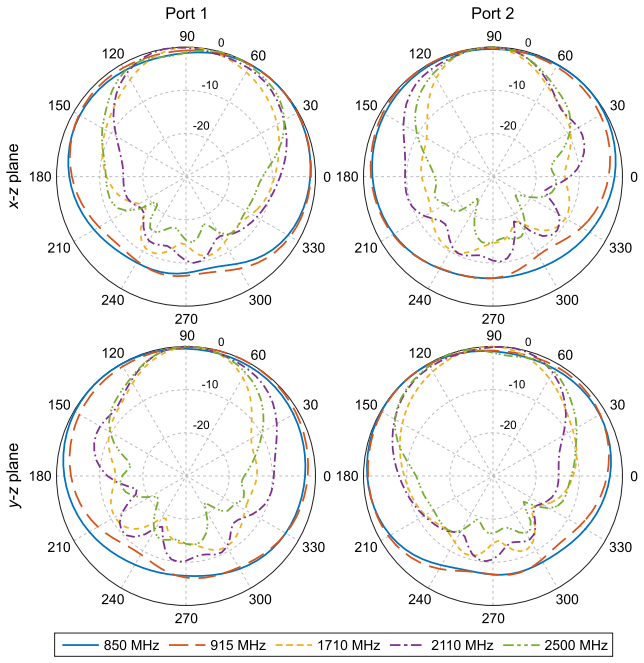

FIGURE 5. Simulated radiation patterns of the proposed 2G/3G/LTE MIMO indoor base station antenna in *x*-*z* and *y*-*z* planes at 850, 915, 1710, 2110, and 2500 MHz.

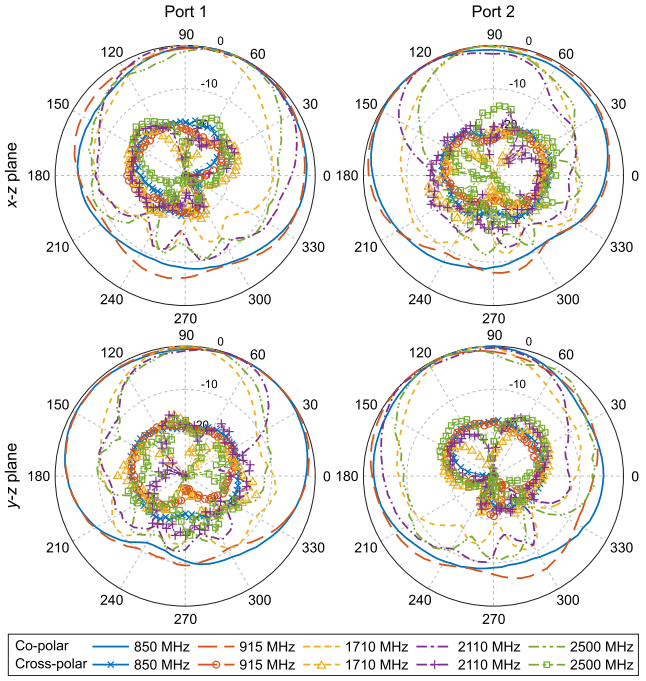

FIGURE 6. Measured radiation patterns for co- and cross- polarizations of the proposed 2G/3G/LTE MIMO indoor base station antenna in *x*-*z* and *y*-*z* planes at 850, 915, 1710, 2110, and 2500 MHz.

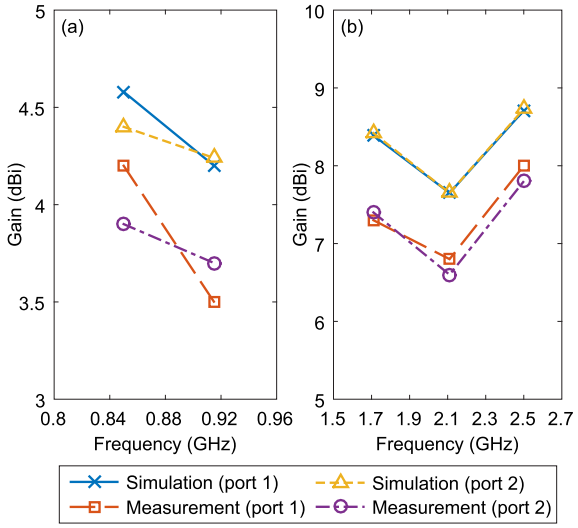

FIGURE 7. Comparison of simulated and measured antenna gains of the proposed 2G/3G/LTE MIMO indoor base station antenna for the (a) lower and (b) upper frequency bands.

The normalized radiation patterns (gain) of the proposed MIMO antenna in *x*-*z* and *y*-*z* planes (see Fig. 1(a)) at five different frequencies from simulations and measurements are shown in Figs. 5 and 6, respectively. It can be seen that the results show relatively good agreement between simulations and measurement. At the lower frequency band, the antenna provides a wide 3-dB beamwidth as a result of the radiations by two lower monopoles, while at higher operating frequencies, the antenna becomes more directive due to the top radiating patch. The radiation patterns are also mirror-symmetric since the two antenna elements are symmetrically arranged on two sides of the metal isolator, as shown in Fig. 1(a). It is also observed in Fig. 6 that the radiation patterns for cross-polarization is about 15 dB lower than the case of co-polarization.

The comparison of simulated and measured antenna gains for both ports of the antenna is plotted in Fig. 7. From simulations, the antenna gain at the lower frequency band is between 4.2 and 4.6 dBi and varies from 7.6 to 8.7 dBi at the upper frequency band, while the measured gains are slightly lower than simulated ones due to the losses in cables,

TABLE 1. Comparison of the proposed antenna with other 2G/3G/LTE antennas.

Reference	Frequency band (MHz)		Bandwidth (%)		HPBW (degree)		Gain (dBi)		Dimensions (mm^3)
	LB	UB	LB	UB	LB	UB	LB	UB	
[9]	800 - 980	1540 - 2860	20 (VSWR $\leqslant$ 1.5)	60 (VSWR $\leqslant$ 1.5)	60	50	8	8	360 × 280 × 46
[10]	790 - 1010	1380 - 2780	24.4 (VSWR $\leqslant$ 2)	67.3 (VSWR $\leqslant$ 2)	70	80	7.2	7.5	200 × 140 × 51
[33]	790 - 1000	1640 - 2760	23.5 (VSWR $\leqslant$ 2)	51 (VSWR $\leqslant$ 2)	69	73	8.6	8.8	140 × 140 × 75
[34]	790 - 960	1710 - 2170	19.4 (VSWR $\leqslant$ 1.5)	23.7 (VSWR $\leqslant$ 1.5)	64.5	66	9.3	9	255 × 255 × 71
[35]	790 - 960	1710 - 2170	19.4 (VSWR $\leqslant$ 1.5)	23.7 (VSWR $\leqslant$ 1.5)	65	65	9.5	9	255 × 255 × 130
[36]	700 - 1180	1670 - 2730	51 (VSWR $\leqslant$ 1.5)	48 (VSWR $\leqslant$ 1.5)	61.5	90	8.4	8.7	290 × 290 × 100
[37]	700 - 1050	1600 - 3000	40 (VSWR $\leqslant$ 2)	60 (VSWR $\leqslant$ 2)	73	65	6	6.7	220 × 220 × 100
Proposed	800 - 960	1700 - 2700	18 (VSWR $\leqslant$ 1.5)	46 (VSWR $\leqslant$ 1.5)	150	70	4.6	8.7	220 × 220 × 42

connectors and the fabrication tolerance. Notice that there exists a reduction in the antenna gain in the middle of the upper frequency band, which is due to the larger size of the U-shaped slot, leading to a larger beam width comparing with two other resonant frequencies in the upper band. Besides, in comparison with simulated gains, the measured gains for two ports are slightly different which may be caused by reflections from connectors etc. during the measurement.

Table 1 shows the comparison of our proposed antenna with other reference 2G/3G/LTE antennas in literature. It can be seen that the proposed antenna has the lowest profile (height) with relatively good performance and satisfies the design requirement for 2G/3G/LTE indoor base stations.

III. PARAMETRIC ANALYSIS

In the previous section, all parameters of the proposed MIMO antenna are optimized ones found in simulations. In this section, we show effects of varying parameters on the performance of the antenna.

A. EFFECT OF THE DISTANCE BETWEEN THE WIDER MONOPOLE AND THE FEEDING PIN

As mentioned earlier, the distance between the feeding pin and the wider monopole is a crucial parameter for having a good impedance matching for the resonance at 950 MHz. In simulations, we choose two additional values of 1.2 mm and 1.4 mm for the gap size, and demonstrate the effect of such variations. Figure 8 shows the calculated S-parameters (S_{11} and S_{21}) with varying gap sizes. It can be observed that when the gap is larger than the optimized value of 1.3 mm, not only the impedance matching at 950 MHz (resonance of the wider monopole) becomes worse (as illustrated in the Smith chart in Fig. 9), the value of S_{11} at around 2500 MHz also increases due to the shift of the resonance of the larger U-shaped slot, which is caused by the change in mutual coupling between the feeding pin and the wider monopole. On the other hand, when the gap size becomes smaller, only S_{11} at the upper frequency band below 2250 MHz is affected, which is also caused by the shift of the resonance of the larger U-shaped slot. Nonetheless, the isolation (S_{21}) is only slightly affected by the change in the gap size. Hence it is important to maintain an accurate gap size during the manufacturing of the antenna.

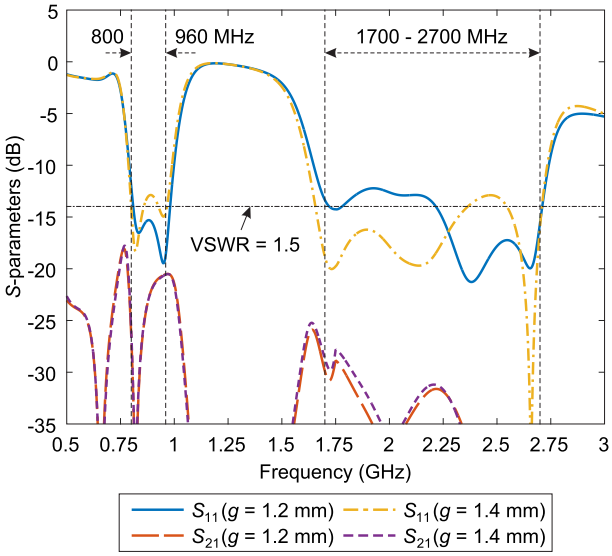

FIGURE 8. Effect of varying the distance between the feeding pin and the wider monopole, g on the S-parameters of the proposed antenna with g = 1.2 mm and g = 1.4 mm.

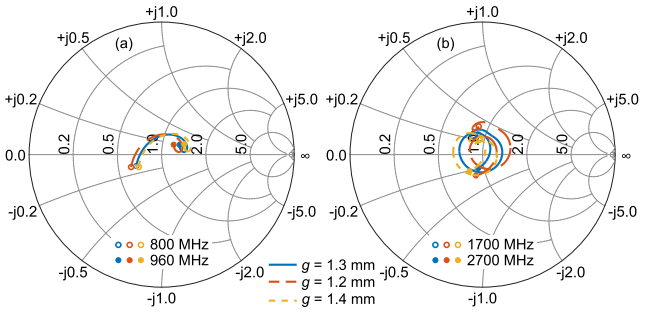

FIGURE 9. Effect of varying the distance between the feeding pin and the wider monopole, g on the impedance matching of the proposed antenna illustrated on Smith chart.

B. EFFECT OF THE ISOLATOR MATERIAL

The main function of the isolator is to reduce mutual coupling between two antenna elements and improve impedance matching, thus an absorber can be also used in place of metal (aluminum). Simulations of the isolator made of

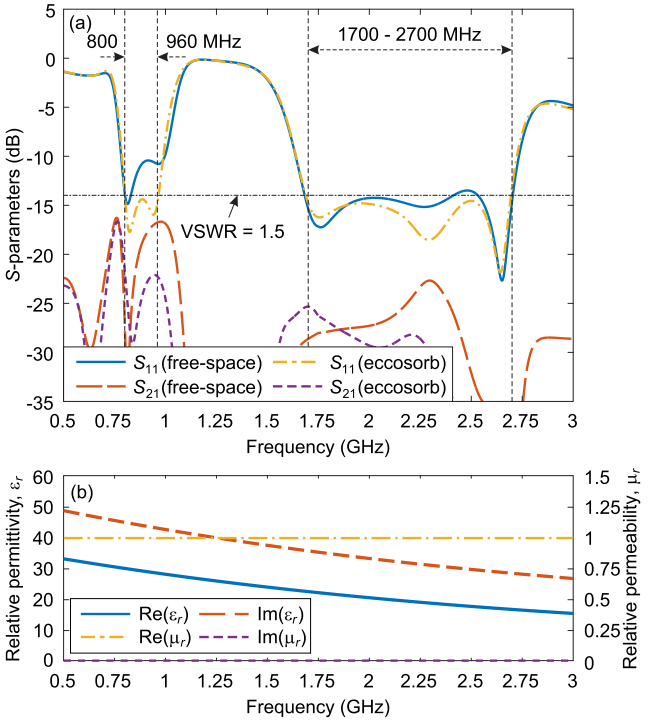

FIGURE 10. (a) Comparison of *S*-parameters when an absorbing material, ECCOSORB QR-13AF is used as the isolator, and the case of without the isolator (free-space). (b) Permittivity and permeability of the absorbing material, ECCOSORB QR-13AF versus frequency.

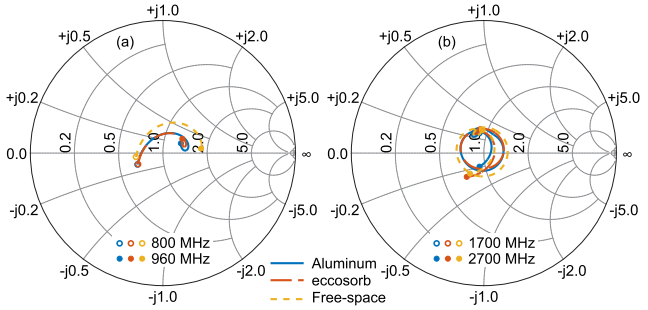

FIGURE 11. Effect of changing the material of the isolator between two antenna elements on the impedance matching of the proposed antenna illustrated on Smith chart.

an absorbing material, ECCOSORB QR-13AF from Laird Technologies [38] (dimensions 240 × 10 × 39.4 mm^3), as well as for the case of without the isolator are performed, with all other parameters of the antenna remain unchanged. The comparison results of these two cases are shown in Fig. 10. It can be seen that the *S*-parameters of the antenna are nearly unchanged when the aluminum isolator is replaced by the absorber, which also validates that a metallic sheet can be used as the isolator. However, the cost of the absorber is much higher than aluminum, and the antenna gain is slightly lower due to the absorption of radiation. For the case of without the isolator (free-space), it is apparent that not only the isolation between two ports of the antenna is reduced, the impedance matching also becomes worse, especially at the lower frequency band as illustrated in the Smith chart in Fig. 11.

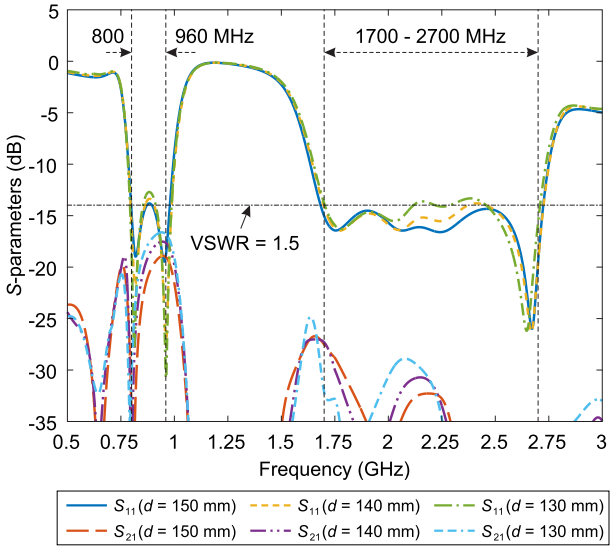

FIGURE 12. Effect of varying the separation distance, *d* between antenna elements: $d = 150$ mm, $d = 140$ mm and $d = 130$ mm on the *S*-parameters of the proposed 2G/3G/LTE MIMO indoor base station antenna.

C. EFFECT OF THE DISTANCE BETWEEN ANTENNA ELEMENTS

In the finalized design shown in Fig. 1, two antenna elements are separated by a maximum distance of 160 mm (while they can still be contained within the radome). It is expected that when the distance is decreased, both isolation between two ports and the return loss will become worse. In simulations, three additional distances: 150, 140, and 130 mm are considered and the comparisons of *S*-parameters for these three cases are shown in Fig. 12. It can be seen that the performance of isolation and impedance matching decreases as the separation distance between antenna elements increases. On the other hand, if it is required to have a better isolation performance during operation, a larger distance between antenna elements can be considered, but the overall size of the MIMO antenna will increase accordingly.

IV. CONCLUSION

In conclusion, we proposed a low-profile indoor MIMO base station antenna for 2G/3G/LTE systems. In order to overcome the challenge of achieving wide bandwidths at both 800 - 960 MHz and 1700 - 2700 MHz simultaneously, we apply the technique of introducing additional resonances. Specifically, for covering the upper frequency band, in addition to the resonance of the microstrip patch antenna, two U-shaped slots are created on the top radiating patch for introducing two more resonances. For the lower frequency band, two folded monopoles are used. Comparing with existing indoor 2G/3G/LTE base station antennas, the main advantages of the proposed design are its simplicity in the antenna feeding structure, low profile as well as the overall low cost. It can be anticipated that the proposed MIMO antenna can find its immediate applications in indoor 2G/3G/LTE mobile networks.

REFERENCES

[1] Z. Zhao, J. Lai, B. Feng, and C.-Y.-D. Sim, "A dual-polarized dual-band antenna with high gain for 2G/3G/LTE indoor communications," *IEEE Access*, vol. 6, pp. 61623–61632, 2018.
[2] H. Wen, Y. Qi, Z. Weng, F. Li, and J. Fan, "A multiband dual-polarized omnidirectional antenna for 2G/3G/LTE applications," *IEEE Antennas Wireless Propag. Lett.*, vol. 17, no. 2, pp. 180–183, Feb. 2018.
[3] J. Lai, B. Feng, Q. Zeng, and S. Su, "A dual-band dual-polarized omnidirectional antenna for 2G/3G/LTE indoor system applications," in *Proc. IEEE Int. Conf. Signal Process., Commun. Comput. (ICSPCC)*, Sep. 2018, pp. 1–3.
[4] X. Bai, M. Su, Y. Liu, and S. Li, "A novel broadband dual-polarized low-profile antenna for 4G LTE applications," in *Proc. IEEE 5th Int. Symp. Electromagn. Compat. (EMC)*, Oct. 2017, pp. 1–3.
[5] X.-W. Dai, Z.-Y. Wang, C.-H. Liang, X. Chen, and L.-T. Wang, "Multiband and dual-polarized omnidirectional antenna for 2G/3G/LTE application," *IEEE Antennas Wireless Propag. Lett.*, vol. 12, pp. 1492–1495, 2013.
[6] L. Zhou, Y.-C. Jiao, Y. Qi, Z. Weng, and T. Ni, "Wideband ceiling mount omnidirectional antenna for indoor distributed antenna system applications," *Electron. Lett.*, vol. 50, no. 4, pp. 253–255, Feb. 2014.
[7] M. Secmen and A. Hizal, "A dual-polarized wide-band patch antenna for indoor mobile communication applications," *Prog. Electromagn. Res.*, vol. 100, pp. 189–200, 2010.
[8] R. Caso, A. A. Serra, M. Pino, P. Nepa, and G. Manara, "A wideband slot-coupled stacked-patch array for wireless communications," *IEEE Antennas Wireless Propag. Lett.*, vol. 8, pp. 986–989, 2010.
[9] Y. Cui, R. Li, and P. Wang, "Novel dual-broadband planar antenna and its array for 2G/3G/LTE base stations," *IEEE Trans. Antennas Propag.*, vol. 61, no. 3, pp. 1132–1139, Mar. 2013.
[10] B. Feng, W. Hong, S. Li, W. An, and S. Yin, "A dual-wideband double-layer magnetoelectric dipole antenna with a modified horned reflector for 2G/3G/LTE applications," *Int. J. Antennas Propag.*, vol. 2013, Nov. 2013, Art. no. 509589.
[11] A. Moradi and T. A. Rahman, "Broadband modified rectangular microstrip patch antenna using stepped cut at four corners method," *Prog. Electromagn. Res.*, vol. 137, pp. 599–619, Mar. 2013.
[12] R. B. Waterhouse, "Broadband stacked shorted patch," *Electron. Lett.*, vol. 35, no. 2, pp. 98–100, Jan. 1999.
[13] J. Ollikainen, M. Fischer, and P. Vainikainen, "Thin dual-resonant stacked shorted patch antenna for mobile communications," *Electron. Lett.*, vol. 35, no. 6, pp. 437–438, Mar. 1999.
[14] G.-Y. Lee, T.-W. Chiou, and K.-L. Wong, "Broadband stacked shorted patch antenna for mobile communication handsets," in *Proc. Asia–Pacific Microw. Conf. (APMC)*, Dec. 2001, pp. 232–235.
[15] R. Li, G. DeJean, M. M. Tentzeris, and J. Laskar, "Development and analysis of a folded shorted-patch antenna with reduced size," *IEEE Trans. Antennas Propag.*, vol. 52, no. 2, pp. 555–562, Feb. 2004.
[16] H.-C. Lien and H.-C. Tsai, "A wide-band circular polarization stacked patch antenna for the wireless communication applications," *Piers Online*, vol. 4, no. 2, pp. 255–258, 2008.
[17] J. A. Ansari and R. B. Ram, "Broadband stacked U-slot microstrip patch antenna," *Prog. Electromagn. Res. Lett.*, vol. 4, pp. 17–24, Jan. 2008.
[18] Z. Wang, S. Fang, and S. Fu, "Broadband stacked patch antenna with low VSWR and low cross-polarization," *ETRI J.*, vol. 32, no. 4, pp. 618–621, Aug. 2010.
[19] M. A. Matin, B. S. Sharif, and C. C. Tsimenidis, "Broadband stacked microstrip antennas with different radiating patch," *Wireless Pers. Commun.*, vol. 56, no. 4, pp. 637–648, Feb. 2011.
[20] M. Clenet, C. B. Ravipati, and L. Shafai, "Bandwidth enhancement of U-slot microstrip antenna using a rectangular stacked patch," *Microw. Opt. Techn. Lett.*, vol. 21, no. 6, pp. 393–395, Jun. 1999.
[21] A. K. Shackelford, K. F. Lee, K. M. Luk, and R. C. Chair, "U-slot patch antenna with shorting pin," *Electron. Lett.*, vol. 37, no. 12, pp. 729–730, Jun. 2001.
[22] V. Natarajan, E. Chettiar, and D. Chatterjee, "An ultra-wideband dual, stacked, U-slot microstrip antenna," *IEEE Antennas Propag. Soc. Symp.*, Jun. 2004, pp. 2939–2942.
[23] L. K. Fong and R. Chair, "On the use of shorting pins in the design of microstrip patch antennas," *Hong Kong Inst. Eng. (HKIE) Trans.*, vol. 11, no. 4, pp. 31–38, Jun. 2004.
[24] K. Kanjanasit, V. Vivek, and N. Homsup, "Novel design of a wideband improved U-slot on rectangular patch using additional loading slots," in *Proc. 2nd Int. ECTI Conf.*, May 2005, pp. 1–4.
[25] G. F. Khodae, J. Nourinia, and C. Ghobadi, "A practical miniaturized U-slot patch antenna with enhanced bandwidth," *Prog. Electromagn. Res. B*, vol. 3, pp. 47–62, 2008.
[26] R. Chair, W. C. Mok, K. M. Luk, and K. F. Lee, "A wideband rectangular patch antenna with shorting pins," *Microw. Opt. Technol. Lett.*, vol. 37, no. 3, pp. 165–167, May 2003.
[27] A. K. Shackelford, K.-F. Lee, and K. M. Luk, "Design of small-size wide-bandwidth microstrip-patch antennas," *IEEE Antennas Propag. Mag.*, vol. 45, no. 1, pp. 75–83, Feb. 2003.
[28] K. Siakavar, *Methods to Design Microstrip Antennas for Modern Applications*. Rijeka, Croatia: InTech, 2011, ch. 9, pp. 173–236.
[29] M. Secmen, "Multiband and wideband antennas for mobile communication systems," in *Recent Developments in Mobile Communications—A Multidisciplinary Approach*. Rijeka, Croatia: InTech, 2011, ch. 8, pp. 143–166.
[30] Y. Zhao, "Dual-wideband microstrip antenna for LTE indoor base stations," *Electron. Lett.*, vol. 52, no. 8, pp. 576–578, Apr. 2016.
[31] C. L. Mak, K. M. Luk, K. F. Lee, and Y. L. Chow, "Experimental study of a microstrip patch antenna with an L-shaped probe," *IEEE Trans. Antennas Propag.*, vol. 48, no. 5, pp. 777–783, May 2000.
[32] K.-M. Luk and H. Wong, "A new wideband unidirectional antenna element," *Int. J. Microw. Opt. Technol.*, vol. 1, no. 1, pp. 35–44, Jun. 2006.
[33] H. Huang, Y. Liu, and S. Gong, "A novel dual-broadband and dual-polarized antenna for 2G/3G/LTE base stations," *IEEE Trans. Antennas Propag.*, vol. 64, no. 9, pp. 4113–4118, Sep. 2016.
[34] G. Cui, S.-G. Zhou, G. Zhao, and S.-X. Gong, "A compact dual-band dual-polarized antenna for base station application," *Prog. Electromagn. Res. C*, vol. 64, pp. 61–70, 2016.
[35] Y. He, W. Tian, and L. Zhang, "A novel dual-broadband dual-polarized electrical downtilt base station antenna for 2G/3G applications," *IEEE Access*, vol. 5, pp. 15241–15249, 2017.
[36] H. Huang, Y. Liu, and S. Gong, "A dual-broadband, dual-polarized base station antenna for 2G/3G/4G applications," *IEEE Antennas Wireless Propag. Lett.*, vol. 16, pp. 1111–1114, 2017.
[37] A. Alieldin, Y. Huang, S. J. Boyes, M. Stanley, S. D. Joseph, and B. Al-Juboori, "A dual-broadband dual-polarized fylfot-shaped antenna for mobile base stations using MIMO over-lapped antenna subarrays," *IEEE Access*, vol. 6, pp. 50260–50271, 2018.
[38] *ECCOSORB QR-13AF*. Accessed: May 20, 2019. [Online]. Available: http://www.eccosorb.com/products-eccosorb-qr13af.htm

YAN ZHAO (M'07–SM'15) received the B.Sc. degree from the Beijing University of Posts and Telecommunications (BUPT), China, the M.Sc. degree from the University of Birmingham, U.K., and the Ph.D. degree from the Queen Mary University of London, U.K.

He is currently an Associate Professor with Chulalongkorn University, Thailand. He has published over 100 technical papers in highly ranked journals and refereed conference proceedings. He has extensive experience in computational electromagnetics, notably in the area of finite-difference time-domain (FDTD) method for metamaterials. He also has experience in the ray tracing technique, the uniform theory of diffraction (UTD), and their applications in antenna engineering and radio propagation.

Dr. Zhao is a founding member of the Innovative Electromagnetic Academic of Thailand (iEMAT), the Chair of the IEEE Thailand Section Joint MTT/APS Chapter, and a Managing Editor of the *Engineering Journal*. He has served as a Regular Reviewer for the IEEE TRANSACTIONS ON ANTENNAS AND PROPAGATIONS, the IEEE ANTENNAS AND WIRELESS PROPAGATION LETTERS, the IEEE MICROWAVE AND WIRELESS COMPONENTS LETTERS, *Progress in Electromagnetics Research*, and *Optics Express*.

CHAWALIT RAKLUEA (GS'17) received the B.Eng. and M.Eng. degrees in electrical engineering (telecommunication) from the King Mongkut's University of Technology North Bangkok (KMUTNB), Thailand, where he is currently pursuing the Ph.D. degree in electrical engineering. He is also a Lecturer with the Rajamangala University of Technology Thanyaburi (RMUTT), Thailand. His research interests include wireless power transmission, metamaterials, metasurface, and antenna technology.

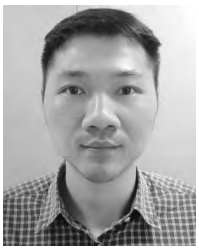

TANAN HONGNARA received the B.Eng., M.Eng, and Ph.D. degrees in electrical engineering from the King Mongkut's University of Technology North Bangkok, Thailand, in 2008, 2012, and 2018, respectively. He was also a Scholarship Student with the cooperation of the King Mongkut's University of Technology North Bangkok and The Thailand Research Fund. He is currently an Engineer with the Department of Telecommunication Research and Development, Denki Kogyo Company Ltd., Japan. His current research interests include metasurface, metamaterial, and base station antenna design.

SARAWUTH CHAIMOOL (M'08–SM'17) received the B.Eng., M.Eng., and Ph.D. degrees in electrical engineering from the King Mongkut's University of Technology North Bangkok (KMUTNB), Thailand, in 2002, 2004, and 2008, respectively.

He was a Lecturer with the Department of Electrical Engineering, KMUTNB, from 2004 to 2014. From 2014 to 2016, he was with Udon Thani Rajabhat University. He was promoted to Assistant Professor and Associate Professor, in 2012 and 2015, respectively. He is currently an Associate Professor with Khon Kaen University, Thailand, and an Associate Researcher under Assoc. Prof. Dr. Y. Zhao with Chulalongkorn University. He has published over 100 technical papers, two-chapter books, and two academic books, including *Antenna Engineering* and *Electromagnetic Engineering*. His current research interests include metamaterials and metasurfaces, wireless power transfer, advanced antenna designs, and passive microwave circuits. Moreover, he teaches and contributes to Youtube (Jaounarak), Facebook (EMETARA), and website (metaradiator).

Dr. Chaimool is a member of ECTI Thailand and EEAAT Thailand. He is also a Founding Member of the Innovative Electromagnetic Academic of Thailand (iEMAT) and an Editor of *Cogent Engineering*.